Synthesis, X-ray Crystallography, and Pharmacokinetics of Novel Azomethine Prodrugs† of (*R*)-α-Methylhistamine:‡ Highly Potent and Selective Histamine H_3 Receptor Agonists

Michael Krause,§ Agnès Rouleau,⊥ Holger Stark,§ Peter Luger,|| Ralph Lipp,§ Monique Garbarg,⊥ Jean-Charles Schwartz,⊥ and Walter Schunack*,§

Institut für Pharmazie and Institut für Kristallographie, Freie Universität Berlin, D-14195 Berlin, Germany, and Unité de Neurobiologie et Pharmacologie, Centre Paul Broca de l'INSERM, F-75014 Paris, France

Received April 24, 1995®

Since various neuroregulatory functions of the histamine H_3 receptor have been proved during the last few years, the H_3 receptor is of current interest. Azomethine derivatives of the highly potent histamine H_3 receptor agonist (*R*)-α-methylhistamine (**1**) were prepared as lipophilic prodrugs to improve the bioavailability of the hydrophilic drug, particularly its entry into the brain. Additionally, azomethine derivatization provides protection against histamine methyltransferase, the major metabolizing enzyme in man, and thus efficiently enhances the bioavailability of **1**. The molecular conformations of (*R*)-2-[[*N*-[1-(1*H*-imidazol-4-yl)-2-propyl]-imino]phenylmethyl]phenol (**9a**) and (*R*)-4-fluoro-2-[[*N*-[1-(1*H*-imidazol-4-yl)-2-propyl]imino]-(4-chlorophenyl)methyl]phenol (**9p**) were determined by X-ray structure analysis. An intramolecular hydrogen bond which is essential for the stability of these azomethines was thereby confirmed. Moreover, the pharmacokinetic parameters of the prodrugs were investigated *in vitro* as well as *in vivo*. The halogenated azomethines have an effect following peroral administration in mice, and some of them seem to be highly potent for the central nervous system (CNS) delivery of **1**. At present the most potent prodrug of **1** is (*R*)-4-chloro-2-[[*N*-[1-(1*H*-imidazol-4-yl)-2-propyl]imino](4-chlorophenyl)methyl]phenol (**9q**), reaching by far the highest CNS level of **1** (c_{max} = 71 ng/g). Prodrugs of this type are not only valuable pharmacological tools but may also become H_3 histaminergic drugs for therapeutic use.

Introduction

The discovery of a third histamine receptor subtype by Arrang *et al.* in 1983 has been a landmark in the field of histamine research.[1] During the past decade the neurotransmitter function of histamine was confirmed by the subsequent development of selective histamine H_3 receptor ligands.[2,3] Histamine H_3 receptors are presynaptically located autoreceptors, the stimulation of which inhibits both the synthesis and the release of neuronal histamine.[4,5] Moreover, H_3 receptors have also been shown to act as heteroreceptors at noradrenergic,[6] cholinergic,[7] dopaminergic,[8] serotonergic,[9] and nonadrenergic noncholinergic (NANC)[10] neurons. Even though they are spread over many peripheral tissues, histamine H_3 receptors are predominantly found in distinct regions of the central nervous system (CNS) in various species, *e.g.*, cerebral cortex, accumbens nucleus, striatum, and substantia nigra.[11-13] A few years ago, the existence of histamine H_3 receptors in human brain was also established.[14]

(*R*)-α-Methylhistamine (1; Figure 1) is a highly selective and potent histamine H_3 receptor agonist which is nowadays used as the standard agonist in pharmacological studies concerning the H_3 receptor.[2,15] However, the fact that **1** shows insufficient peroral absorption, poor brain penetration, and rapid metabolism in man[16] limits its pharmacological and its potential clinical use for CNS disorders like somnipathy.[17] Additionally, peripheral indications for H_3 receptor agonists like inflammation or asthma have been suggested more recently.[18,19] Because of its high polarity and strong basicity, **1** poorly penetrates biological membranes, especially the blood-brain barrier (BBB) even after iv administration of high doses.[20] Histamine which has a closely related structure to **1** does not cross the BBB at all,[21,22] and for that reason neuronal histamine has to be synthesized from L-histidine in histaminergic neurons. On account of their chemical similarities, one may suggest that 1 has similar pK_a values to histamine. The side chain nitrogen of histamine has a pK_a value of 9.4 at 37 °C,[23] and consequently the monocation of 1 ought to predominate in human plasma (>95%).

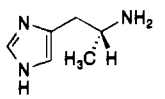

Figure 1. (*R*)-α-Methylhistamine (1).

Furthermore 1 is a good substrate for histamine methyltransferase (HMT),[24] a major histamine metabolizing enzyme in man, which accounts for the short half-life and poor bioavailability of **1** in this species.[16]

It has thus been the aim of the present study to design lipophilic, nonbasic prodrugs of **1** to overcome its disadvantageous pharmacokinetics. Therefore bioreversible azomethine derivatives of **1** were prepared by coupling its primary amine functionality to several aromatic ketones.[25] On the one hand, the nonbasic

† Presented in part: New Perspectives in Histamine Research, Satellite Symposium of the XIIth International Congress of Pharmacology of IUPHAR, Winnipeg, Canada, July 20-24, 1994, International Symposium on Medicinal Chemistry (Abstract P 330), Paris, France, September 19-23, 1994, and PCT Int. Appl.[25]

‡ Nomenclature of substituted histamine derivatives is based on the method of Black and Ganellin.[50]

* Author to whom correspondence should be addressed.

§ Institut für Pharmazie, Freie Universität Berlin, Königin-Luise-Strasse 2+4.

⊥ Centre Paul Broca de l'INSERM, 2ter rue d'Alésia.

|| Institut für Kristallographie, Freie Universität Berlin, Takustrasse 6.

® Abstract published in *Advance ACS Abstracts*, September 1, 1995.

0022-2623/95/1838-4070$09.00/0

azomethine double bond should mask the basic amine under physiological conditions and prevent its recognition by the metabolizing enzyme, and on the other hand, the aryl residues should increase the lipophilicity of the resulting prodrugs. However, this prodrug approach has successfully been used for the CNS delivery of the antiepileptic progabide (Gabren) which contains the same promoiety as **9p**.[26,27] In the meantime several azomethine derivatives of GABA mimetics and other primary amines were prepared.[28,29] Anyway, since this method was previously used to provide lipophilicity to agents not entering the brain easily, it has to be emphasized that azomethine derivatization of **1** also provides protection against metabolization by HMT.

In order to optimize the pharmacokinetic profile of these azomethines, the substitution pattern of the promoiety was altered in an attempt to influence both the penetration of biological membranes and the rate of conversion. Hence a balance had to be found between hydrolytic stability and lability, which mainly determines the rate of drug liberation, and between lipophilicity and hydrophilicity, which mainly determines the penetration of biological membranes. The designed azomethine prodrugs were tested *in vitro* to mimic physiological conversion to the active drug **1** and *in vivo* after peroral administration to mice. As a result, it was observed that some of the described azomethine prodrugs are very effective following peroral application for the delivery of **1** into the CNS and that their pharmacokinetics strongly depend on the substituents of the aromatic residues.

In conclusion the pharmacokinetic properties of the prodrugs can be shifted to the desired direction by varying the substitution pattern of the promoiety.

Chemistry

Two chemical classes of compounds were synthesized in this study. Derivatives of 2-hydroxybenzophenone **4** readily condensed with **1** to give the desired azomethines **9** (Scheme 1). These prodrugs have a greatly increased lipophilicity and a considerably reduced basicity. Furthermore, due to an intramolecular hydrogen bond between the phenolic hydroxyl group and the imine nitrogen, they show a sufficient hydrolysis rate in aqueous solution under both *in vitro* and *in vivo* conditions. This hydrogen bond not only increases stability but also facilitates the formation of the carbon–nitrogen double bond. The stereochemical conformations of **9a,p** were confirmed by X-ray crystallography, and these served as reference compounds for all the described azomethines. Moreover azomethine derivatization of compounds that comprise a primary amine functionality could be a useful protection to mask basicity and reduce polarity. Though similar approaches have been reviewed by Green and Wuts,[30] only a few of them have been used extensively. High yields in preparation and quantitative cleavage under mild conditions make 2-hydroxybenzophenone and its derivatives useful protective groups in organic synthesis.

However, when **1** was treated with monoaryl carbonyl components, the respective isomeric 1,2,3,4-tetrahydro-1*H*-imidazo[4,5-*c*]pyridine derivatives called spinaceamines (**11**) were obtained, as a result of a ring closure reaction, instead of the desired azomethines (Table 2).

Synthesis. The azomethine prodrugs **9** were synthesized according to Scheme 1. The precursors that

Scheme 1. General Synthesis of Diaryl Azomethine Prodrugs of **1**[a]

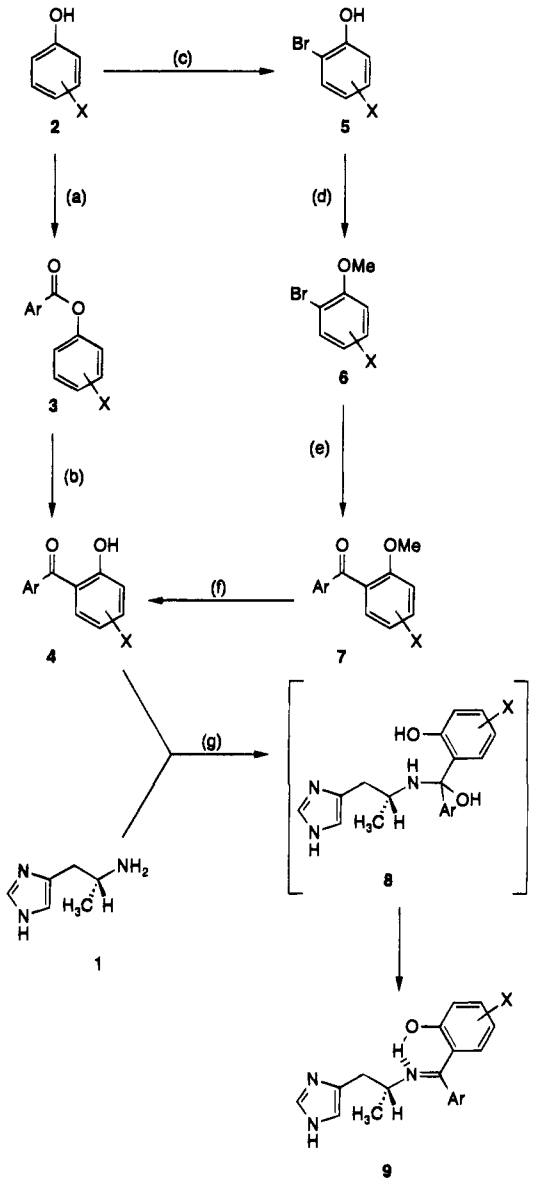

[a] Reagents: (a) ArCOCl, Et_3N/Et_2O, 1 h reflux; (b) $AlCl_3$, 200 °C for 20 min; (c) Br_2/CCl_4, 0–5 °C for 2 h, then 18 h room temperature; (d) MeONa, Me_2SO_4, 12 h reflux; (e) Mg, $ArCN/Et_2O$, 2 h reflux; (f) BBr_3/CH_2Cl_2, 12 h room temperature; (g) EtOH or MeCN, 18 h reflux with repeated evaporation.

are not purchasable were obtained as previously described in a Fries rearrangement of phenolic esters **3** which is the most likely method to prepare the corresponding 2-hydroxybenzophenone derivatives **4**.[31,32] The esters **3** were prepared in a slightly modified procedure, according to Einhorn, by using Et_3N instead of pyridine.[33] An alternative is the Grignard reaction that starts from *o*-brominated anisole derivatives[34] **6** with benzonitriles[35] and the subsequent cleavage of the 2-methoxybenzophenones **7** with BBr_3[36] to give **4**.

Compound **1** was liberated from its dihydrogen maleate by a basic anion exchange with Amberlite IRA 400 for the condensation reaction. After refluxing **1** and **4** in dry acetonitrile or ethanol and subsequent azeotropic distillation of the solvent, the diaryl azomethines **9a–r** (Table 1) were obtained in high yields (up to 91%) via initially formed hemiaminals **8** which were not separated. Compounds **9a–r** show maxima in UV absorp-

Table 1. Synthetic and Physicochemical Data of Azomethine Prodrugs of 1 Prepared for This Study[a]

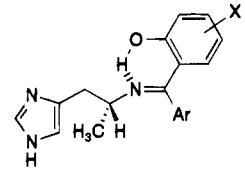

no.	Ar	X	yield (%)	$[\alpha]^{20}_D$[b] (deg)	λ_{max} (nm)	mp (°C)	formula	M_r
9a	Ph	H	85	−295.4	399	134−136	$C_{19}H_{19}N_3O$	305.4
9b	2-HOPh	H	82	−154.9	398	281−283	$C_{19}H_{19}N_3O_2$	321.4
9c	Ph	5-OH	45	−290.5	378	238[c]	$C_{19}H_{19}N_3O_2$	321.4
9d	Ph	5-OMe	46	−478.0	380	152	$C_{20}H_{21}N_3O_2$	335.4
9e	Ph	4-Me	86	−265.5	412	117	$C_{20}H_{21}N_3O$	319.4
9f	Ph	4-F	82	−247.7	414	170	$C_{19}H_{18}FN_3O$	323.4
9g	Ph	4-Cl	88	−237.6	414	156	$C_{19}H_{18}ClN_3O$	339.8
9h	Ph	4-Br	90	−188.5	414	165	$C_{19}H_{18}BrN_3O$	384.3
9i	Ph	4-Cl, 5-Me	47	−246.2	410	86	$C_{20}H_{20}ClN_3O{\cdot}0.5H_2O$	362.9
9k	Ph	6-Cl, 4-F	79	−400.2	422	139	$C_{19}H_{17}ClFN_3O$	357.8
9l	4-FPh	H	85	−246.3	402	133	$C_{19}H_{18}FN_3O$	323.4
9m	4-ClPh	H	62	−218.2	404	109−110	$C_{19}H_{18}ClN_3O$	339.8
9n	4-FPh	4-F	62	−210.8	414	158	$C_{19}H_{17}F_2N_3O$	341.4
9o	4-FPh	4-Cl	91	−224.5	412	164	$C_{19}H_{17}ClFN_3O$	357.8
9p	4-ClPh	4-F	85	−195.5	416	126	$C_{19}H_{17}ClFN_3O$	357.8
9q	4-ClPh	4-Cl	84	−189.4	412	144	$C_{19}H_{17}Cl_2N_3O$	374.3
9r	1-naphthyl	4-F	84	−171.0	412	209−211	$C_{23}H_{20}FN_3O{\cdot}0.25H_2O$	373.4

[a] All compounds were analyzed for C, H, and N and are within ±0.4% of the theoretical values. [b] c = 10 mg/mL in MeOH. [c] Decomposition.

Table 2. Synthetic and Physicochemical Properties of Spinaceamine Derivatives of 1

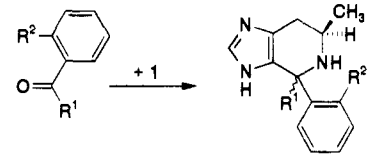

10 11

no.	R^1	R^2	$[\alpha]^{20}_D$[a] (deg)	yield (%)	mp (°C)	formula	M_r
11a	H	H	−46.8	55	220−222	$C_{13}H_{15}N_3{\cdot}0.5H_2O$	222.3
11b	H	OH	+101.5	93	213−215	$C_{13}H_{15}N_3O$	229.3
11c	Me	OH	+104.6	42	175	$C_{14}H_{17}N_3O{\cdot}H_2O$	261.3

[a] c = 10 mg/mL in MeOH.

tion between 375 and 425 nm according to their polymethine structure, so that all of the azomethines are light yellow-colored compounds. Racemization by an imine−enamine tautomerism did not take place as confirmed by optical and X-ray structure analysis. Structures of all compounds were confirmed by ^{1}H-NMR spectra and elemental analysis (C, H, N) in addition to IR and mass spectra (results of the latter not shown). IR and ^{1}H-NMR data gave first indication of an intramolecular hydrogen bond between the azomethine nitrogen and the phenolic hydroxyl group. The chemical shift of the hydroxyl proton in ^{1}H-NMR spectra (δ = 11.75) was independent of the concentration of the azomethine. This indicated intramolecular rather than intermolecular hydrogen bonding. To supply proof of this hypothesis and to determine the stereochemical conformation of two typical azomethines (**9a**,**p**), these compounds were analyzed by X-ray crystallography. With regard to the pharmacokinetic parameters, all of the azomethines were investigated by reversed phase TLC determining their relative lipophilicity compared to **9a**. As it was expected, dihalogenation enhanced the lipophilicity more significantly than monohalogenation, while chlorination was slightly more effective than fluorination.

The monoarylcarbonyl components benzaldehyde, salicylaldehyde, or 2-hydroxyacetophenone (**10a**−**c**), however, yielded colorless spinaceamine derivatives **11a**−**c** with **1** under the above reaction conditions since they underwent an intramolecular ring closure reaction (Table 2). A similar cyclization comparable to the Pictet−Spengler reaction[37] was previously described for histamine and its derivatives by Heyl *et al.*[38] and was further investigated by Stocker *et al.*[39] and Emmett *et al.*[40] In contrast to the azomethines, the isomeric spinaceamines are stable against hydrolysis and hydrogenation. Nevertheless the corresponding azomethines of **11a**−**c** were detectable in solution by TLC. They could even be separated from the spinaceamines by chromatography as long as they were in solution, but it was impossible to isolate them as solid compounds without producing an impurity of **11a**−**c**, respectively.

These results indicate that the spinaceamines seem to be the preferred products of a condensation reaction of **1** with sterically less hindered carbonyl components as compared to the diaryl ketones that preferably form azomethines.

X-ray Structure Analysis. The crystal structures of **9a**,**p** were determined by X-ray analysis as references for the general conformation of **9a**−**r** (for details, see

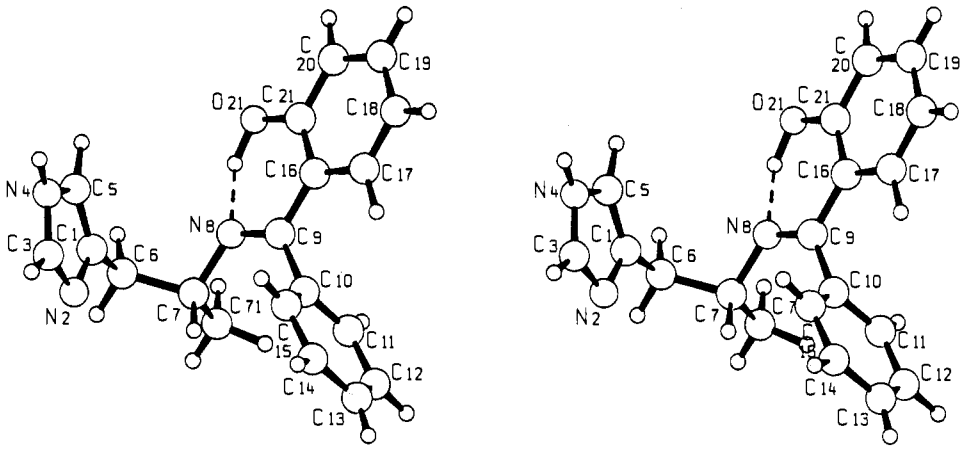

Figure 2. Stereorepresentation of the molecular structure of **9a** as derived from the X-ray analysis.

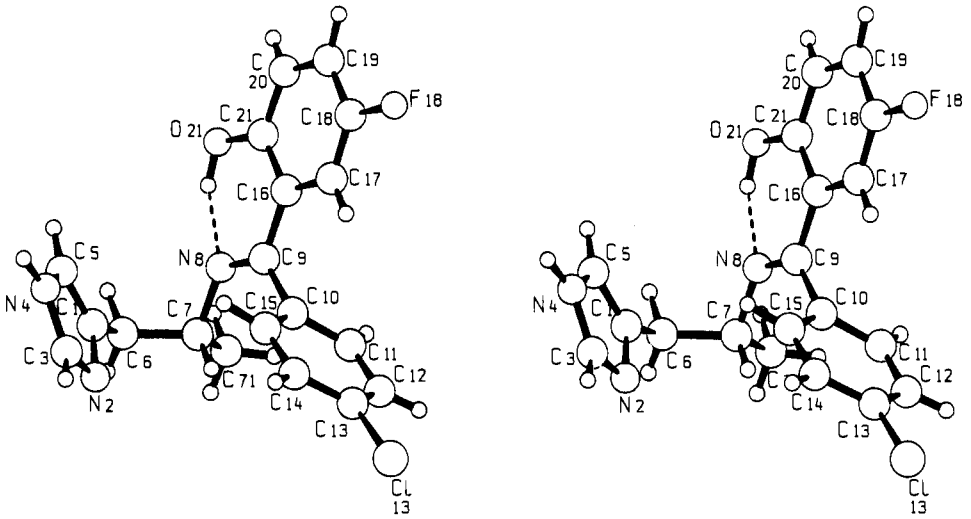

Figure 3. Stereorepresentation of the molecular structure of **9p** as derived from the X-ray analysis.

the Experimental Section). The results are illustrated in Figures 2 and 3 which were drawn with the graphics program SCHAKAL.[41] The molecular structures of **9a,p** are shown in stereorepresentations in which the atomic numbering scheme is also given.

Since the *R*-configuration of the α-carbon atom C(7) was known from the synthesis, only relative structures had to be derived with the configurations assigned in Figures 2 and 3. The molecular structures of **9a,p** are almost alike, and so the following discussion can be applied to both.

A major question of this structure analysis was the existence of an intramolecular hydrogen bond. It is present as O(21)−H(21)···N(8) with distances O···N = 2.542(4)/2.552(3) Å and H···O = 1.71(4)/1.67(4) Å (for **9a/p**). This hydrogen bond causes the phenyl ring C(16)···C(21) to be nearly coplanar with the structural fragment of the N(8)−C(9) double bond. The interplanar angle between the least-squares planes through C(16)···C(21) (mean deviation of contributing atoms σ = 0.005/0.004 Å) and the corresponding plane through N(8), C(9), C(7), C(10), and C(16) (σ = 0.004/0.004 Å) is 7.6(2)° for **9a** and only 1.1(1)° for **9p**. The second phenyl ring C(10)···C(15), however, is almost perpendicularly arranged. Its least-squares plane (σ = 0.006/0.004 Å) forms an angle of 95.1(2)/92.4(2)° with the other phenyl ring plane.

It is interesting to note that the methylhistamine fragments of **9a,p** have a totally different side chain conformation compared to the previously investigated (α*R*,β*S*)-α,β-dimethylhistamine dication,[42] although both α-carbon atoms are in the same *R*-configuration. The side chain conformation can be described by the two torsion angles τ_1 = N(2)−C(1)−C(6)−C(7) and τ_2 = C(1)−C(6)−C(7)−N(8) which are determined as τ_1 = −75.0(5)/−70.4(4)° and τ_2 = −69.5(4)/−68.4(4)° for **9a/p**. For the (α*R*,β*S*)-α,β-dimethylhistamine dication, these angles were ca. τ_1 = 82° and τ_2 = 64°, hence, both of opposite sign. The opposite sign of τ_2 causes the imidazole ring of (α*R*,β*S*)-α,β-dimethylhistamine to be arranged differently from that of both **9a,p**. With respect to Figures 2 and 3, the imidazole is directed up forward for **9a,p** but orientated back downward for the dication.

Not only the molecular structures but also the crystal lattices of **9a,p** are nearly identical. In addition to the above-mentioned intramolecular hydrogen bond, an intermolecular bond, N(4)−H(4)···HN(2)′, exists for **9a/p** [N···N = 2.935(5)/3.052(4) Å, H···N = 1.96(3)/2.11(4) Å; symmetry operation for N(2)′: $^3/_2 - x$, $1 - y$, $-^1/_2 + z$/$-x$, $^1/_2 + y$, $^1/_2 - z$]. The connection is generated via the 2-fold screw axis running in the *z*-direction for **9a** and in the *y*-direction for **9p**. Consequently, endless molecular chains are formed in these directions with the imidazole rings and their hydrogen bonds situated closely to the screw axes. Furthermore, an interdigitated arrangement of phenyl rings belonging to adjacent molecules was observed, but there was no connection

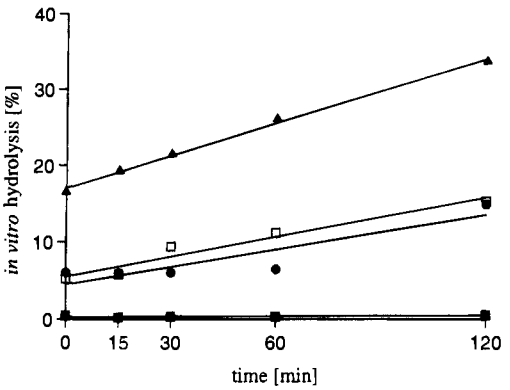

Figure 4. *In vitro* hydrolysis rates in neutral medium (pH = 7.4) at room temperature of prodrugs **9a** (●; slope of the curve, 0.076; $r = 0.9049$), **9f** (□; slope of the curve, 0.086; $r = 0.9762$), **9n** (▲; slope of the curve, 0.143; $r = 0.9980$), and **9r** (■; slope of the curve, 0.02; $r = 0.6240$) determined as free **1**.

recognized between different hydrogen-bonded chains (crystal structures not shown).

Comparing the obtained data of **9a,p** with previously investigated crystalline histamine base, it is noteworthy that both **9a,p** possess the imidazole rings in the N^{τ}-H tautomeric form which is opposite to that reported for histamine (N^{π}-H tautomer).[43] Additionally, the intermolecular hydrogen bond found here is contrary to that in histamine free base which involves the N^{π}-H function of the imidazole ring with the amino group on the side chain of an adjacent molecule.

Pharmacological Results and Discussion

***In Vitro* Results.** The parent compound of this series of azomethines (**9a**) was investigated for its *in vitro* H_3 receptor activity at synaptosomes of rat brain cortex.[44] Compound **9a** (1 μM) which was tested under these conditions as an agonist and as an antagonist in the presence of 1 μM histamine was ineffective at the [^{3}H]histamine release from synaptosomes of rat brain slices.[16] Hence, it follows that only the liberated amine **1** produces the agonistic effect of the described prodrugs at H_3 receptors *in vivo*. Additionally, we discovered that in contrast to **1**, compound **9a** is no longer a substrate for histamine methyltransferase.[16]

The *in vitro* results, shown in Figure 4 and Table 3, indicate that the conversion rates of the azomethines strongly depend on the substitution pattern of the promoiety in neutral and acidic media, respectively. Moreover, the hydrolysis process is essentially a chemical rather than an enzymatic one as shown by the similarity of hydrolysis rates obtained in the presence or absence of tissue extracts.[16] Figure 4 illustrates the effects of electron-withdrawing and bulky substituents with each selected compound (**9a,f,n,r**) representing a different type of substitution pattern. It has to be noted that the level of **1** at $t = 0$ reflects the amount generated during the 30 min derivatization step, performed in highly acidic medium (for details, see the Experimental Section). Replacing the unsubstituted phenyl ring of **9a** by a naphthyl ring (**9r**) decreased the hydrolysis rate by about 90% (pH = 7.4). This may be due to steric hindrance of the carbon–nitrogen double bond by the bulkier naphthyl ring which hampers the addition of water and the subsequent hydrolysis. Thus **9r** was presumed to be too stable *in vivo*. To decrease the hydrolytic stability of **9a**, at first electron-withdrawing halogen substituents were introduced into the promoiety. Monohalogenation of the phenol ring, however, did not produce a pronounced effect as represented by the conversion rate of the monofluoro derivative **9f**. Nevertheless the introduction of a second electron-withdrawing fluorine (**9n**), considerably increased the hydrolysis rate compared to **9a**, although the effect mediated by chlorination was not pronounced to such an extent (Table 3). Including their greater lipophilicity, the dihalogenated azomethines were thus expected to have suitable kinetic parameters *in vivo*. However, these *in vitro* results gave first indications for the evaluation of the prodrug properties.

The spinaceamines **11a–c** did not liberate **1** under these conditions, and since they were found to be stable against hydrolysis, they were suggested to have no prodrug effect *in vivo*.

***In Vivo* Results.** The radioimmunologic determination of **1** by a specific RIA in plasma and the cerebral cortex, in addition to the possibility of quantitative cleavage of the prodrugs, allowed the investigation of

Table 3. Hydrolytic and Pharmacokinetic Data of Prodrugs of **1** Prepared for This Study

	conversion rate (%)					
	in vitro[a] after 2 h		plasma[b] after	$AUC_{plasma}(1)$	$AUC_{CNS}(1)$	CNS ratio of 1, $AUC_{CNS}(1)/AUC_{plasma}(1)$ (%)
no.	pH 1	pH 7.4	6 h	(ng·h/mL)	(ng·h/g)	
9a	14.1	15.0	14	186	nd[c]	
9b	nh[d]	nh		61	nd	
9c	1.7	2.0	1	59	nd	
9d	3.0	6.0		nd	nd	
9e	11.9	16.0	29	141	nd	
9f	30.0	15.4	24	1182	9	0.8
9g	46.9	23.2	33	357	nd	
9h	34.6	16.6	31	279	3.5	1.3
9i	5.6	2.8	41	58	nd	
9k	79.3	19.6	28	94	11	11.7
9l	20.1	18.8	26	238	3	1.3
9m	18.3	13.6	28	249	25	10.0
9n	63.8	33.8	45	296	32	10.8
9o	67.1	26.0	40	230	33	14.3
9p	62.0	15.2	42	387	55	14.2
9q	62.7	16.2	58	361	80	22.1
9r	0.2	1.3	11	23	nd	
11b	0.2	1.3	nd	nd	nd	

[a] Determined as free **1**. [b] $AUC_{plasma}(1)/[AUC_{plasma}(1) + AUC_{plasma}(\mathbf{9})]$, AUC(**9**) is equivalent to **1** comprised in the prodrug. [c] nd = not detectable. [d] nh = not hydrolyzable.

the pharmacokinetic profile of prodrug and drug, respectively. In particular, the amount of free **1** was measured in the blood and tissue samples, while the total amount of **1** was determined in a second aliquot after quantitative hydrolysis of the prodrug. Subsequently the prodrug level was calculated as the difference between these two determinations (for details, see the Experimental Section). But since the pharmacological evaluation of the prodrugs *in vivo* was focused on the central effects of the free drug **1**, several pharmacokinetic parameters, *e.g.*, bioavailability, distribution, metabolism, and elimination, were not considered for this pharmacological screening. These data remain to be determined for the most potent compounds that will finally go into drug development.

At first, the prodrugs were rapidly absorbed after peroral administration as their maximum concentrations were reached after 0.5 h. The *in vivo* conversion rates of the azomethines correlated well with the estimated electronic and steric parameters as was observed *in vitro*. Electron-donating substituents, such as hydroxy or methoxy groups (**9b–d**), and the bulky naphthyl ring (**9r**) decreased the conversion to **1** such that only lower plasma levels compared to **9a** were observed (Table 3). As expected from TLC and the *in vitro* data, the halogenated prodrugs **9f–q** showed higher levels of **1** in the blood and cerebral cortex samples.

Although the reference compound **9a** reached sufficient plasma levels, no CNS level of **1** was measurable by the above RIA after peroral administration. Compound **9a** penetrated to some minimal extent the BBB, though the appearance of **1** in the cerebral cortex was only indirectly detectable. In addition to the assay mentioned above, the main histamine metabolite N^{τ}-methylhistamine is also detectable in a specific RIA. The CNS level of N^{τ}-methylhistamine was significantly reduced by **1** liberated from **9a** as a result of H_3 receptor stimulation. The effect of **9a** was even more pronounced when the [^{3}H]histamine level in brain is considered,[16] presumably because of some cross-reaction of the main metabolite of **1**, (*R*)-α,N^{τ}-dimethylhistamine, and N^{τ}-methylhistamine in the RIA of the latter.[45,46]

However, the introduction of lipophilicity-enhancing halogen substituents led to a striking increase of potency. For the first time, detectable concentrations of **1** in the CNS were observed after peroral administration of halogenated prodrugs. Figures 5 and 6 show the subsequent increase of the prodrugs and **1** in the cerebral cortex achieved by systematic variation of the promoiety substituents. Monofluorination in the phenolic residue (**9f**) resulted in a moderate increase of brain penetration compared to **9a**. Further improvement was achieved by additional fluorination (**9n**) or chlorination (**9p**) at the second phenyl ring. Finally, dichlorination (**9q**) proved to be most effective for the CNS delivery of 1. Not only the highest CNS level but also the highest ratio of CNS to plasma level were observed for **9q** (Table 3).

Interestingly, the plasma levels of 1 did not correlate in any case with the CNS levels. In particular **9f** reached the highest plasma levels in this series, whereas its brain penetration was observed to be relatively low. Additional fluorination in the second phenyl ring (**9n**), however, led to a marked decrease of the plasma level,

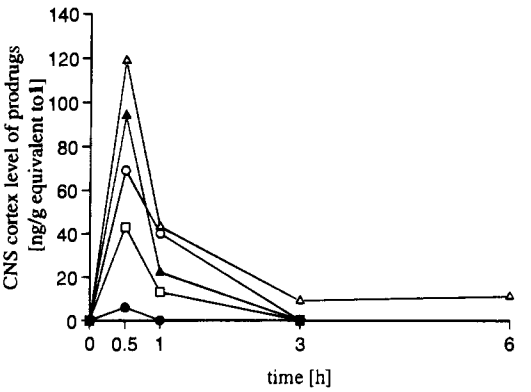

Figure 5. Cerebral cortex levels of prodrugs after peroral administration of **9a** (●), **9f** (□), **9n** (▲), **9p** (○), and **9q** (△) at a dose equivalent of 24 μmol of 1/kg to mice. Prodrug levels are expressed in ng equivalent to 1/g of tissue. Error bars are omitted for sake of clarity.

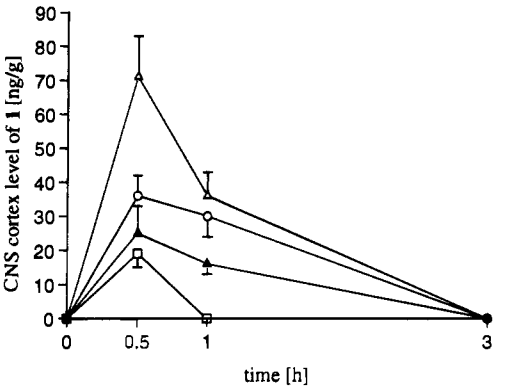

Figure 6. Cerebral cortex levels of 1 after peroral administration of prodrugs **9f** (□), **9n** (▲), **9p** (○), and **9q** (△) at a dose equivalent of 24 μmol of 1/kg to mice; 1 was not detectable after peroral administration of **9a**.

which is about 4 times lower compared to that of **9f**, but conversely led to a 3-fold increase of the CNS level of **1**. These differences between peroral absorption and CNS penetration may reflect the differences between gastrointestinal mucosa and BBB and their sensitivity to slight chemical modifications. As a result, an azomethine prodrug like **9f** may be suitable for peripheral targeting of **1**, whereas **9q** is suitable for central targeting. In general, drug targeting to the periphery as well as into the CNS seems to be possible by varying the substitution pattern of azomethine prodrugs.

Corresponding to the *in vitro* results, the tested spinaceamine **11b** did not show detectable levels of **1** in neither plasma nor CNS.

Conclusions

In the present study it has been shown that azomethine derivatization is a fruitful approach of prodrug for the histamine H_3 receptor agonist (*R*)-α-methylhistamine (**1**). Firstly, 2-hydroxybenzophenones are proposed to be new principles for protective groups in organic synthesis, but since this work was focused on medicinal chemistry, pharmacokinetic parameters of the prodrugs were mainly investigated. As suggested by the *in vitro* data, these compounds are stable enough in the digestive tract to be perorally administered. Furthermore, they are rapidly absorbed (t_{max} = 0.5 h), and most of them penetrate easily from the plasma into the CNS. In addition azomethine protection enhances efficiently

the bioavailability of **1** by about 200 times in man,[16] proving the success of this approach. With regard to structure–activity relationships, halogenation of the promoiety proved to be most effective for the CNS delivery of **1**. Chlorination seemed to be more effective than fluorination. Particularly **9q** shows an optimal pharmacokinetic profile of this series of azomethine prodrugs. Unexpectedly the monofluoro derivative **9f** showed higher plasma levels than any other azomethine combined with relative low brain penetration, and therefore it could be useful for peripheral targeting of **1**. At present these prodrugs are already valuable pharmacological tools for experimental characterization of neuronal functions of histamine H_3 receptors, and since a similar GABAergic prodrug (progabide, Gabren) has been in therapeutic use as an antiepileptic in France,[27] the clinical use of histamine H_3 receptor agonists for CNS disorders may be achieved with these azomethine prodrugs of **1**. However, the much higher potency of **1** compared to the GABAergic drug (by 3 orders of magnitude) ought to result in lower dosage combined with minimal side effects of the described azomethine prodrugs. Particularly the problematical liberation of high quantities of the halogenated promoiety, which could be the reason for the hepatotoxicity of progabide, should not appear with comparable prodrugs of **1**. A possible indication of centrally active H_3 histaminergic drugs like **9q** may be somnipathy,[17] whereas a peripherally active compound like **9f** may possibly be effective for the treatment of asthma or inflammation.[18,19] In addition this prodrug approach could be generally useful for drug targeting of pharmaceutical compounds possessing a primary amine functionality because limited membrane penetration is often a common problem with primary amines.

Experimental Section

Chemistry. General Procedures. Melting points were determined on an Electrothermal IA 9000 digital melting point apparatus or a Büchi 512 apparatus and are uncorrected. ^{1}H-NMR spectra were recorded on a Bruker AC 300 (300 MHz) spectrometer. Chemical shifts are expressed in ppm downfield from internal Me_4Si as reference. ^{1}H-NMR data are reported in order: multiplicity (br, broad; s, singlet; d, doublet; t, triplet; m, multiplet; asterisk, exchangeable by D_2O), number of protons, and approximate coupling constants in hertz. Optical rotation was determined on a Perkin-Elmer 241 MC polarimeter. A Perkin-Elmer Lambda 15 UV/vis spectrophotometer was used. Elemental analyses (C, H, N) were measured on a Perkin-Elmer 240 B or C instrument and are within ±0.4% of the theoretical values. TLC was performed on silica gel F_{254} plates (Merck). Column chromatography was carried out using silica gel 63–200 μm (Machery & Nagel). Preparative, centrifugally accelerated, radial thin layer chromatography was performed using a Chromatotron 7924T instrument (Harrison Research) and glass rotors with 4 mm layers of silica gel 60 PF_{254} containing gypsum (Merck).

The procedure for the preparation of ketones **3** by a Fries rearrangement of phenolic esters **2** previously described by Kaplan *et al.*[26] was only slightly modified in order to optimize the yields. The optimal amount of catalyst was found to be 1.2 mol of $AlCl_3$/1 mol of **2**. Purification was achieved by either extraction with 2 N NaOH or column chromatography [eluent: CH_2Cl_2 (50%), light petroleum (bp 50–70 °C, 50%)].

General Procedures for Preparation of Azomethines 9. Method A. A solution of 1 (0.25 g, 2 mmol) and an equimolar amount of **4** (2 mmol) in 10 mL of dry EtOH was evaporated to dryness under reduced pressure at 50 °C. This procedure was repeated at least three times until the condensation was completed (TLC). The yellow oil obtained was purified by preparative rotatory chromatography [eluent: CH_2Cl_2 (95–90%), MeOH (5–10%)] and crystallized from dry Et_2O or EtOAc/C_6H_{12} to give **9** as a yellow solid.

Method B. A solution of 1 (0.25 g, 2 mmol) and an equimolar amount of **4** (2 mmol) in 40 mL of dry MeCN was refluxed for 24 h and then evaporated to dryness under reduced pressure at 70 °C. The yellow oil obtained was purified as described under method A.

(*R*)-(−)-2-[[*N*-[1-(1*H*-Imidazol-4-yl)-2-propyl]imino]phenylmethyl]phenol (9a): method A (yield 35%) or method B (yield 85%); crystallized from EtOAc/C_6H_{12}; ^{1}H-NMR (DMSO-d_6) δ 15.63 (s*, 1H, NH), 11.73 (br*, 1H, OH), 7.53 (m, 4H, Ph-2-H, Ph-4-H, Ph-6-H, imidazole-2-H), 7.26 (m, 3H, Ph-3-H, Ph-5-H, HOPh-5-*H*), 6.74 (m, 4H, HOPh-3-*H*, HOPh-4-*H*, HOPh-6-*H*, imidazole-5-H), 3.53 (m, 1H, CH), 2.73 (d, 2H, J = 6, CH_2), 1.15 (d, 3H, J = 6, CH_3). Anal. ($C_{19}H_{19}N_3O$) C, H, N.

(*R*)-(−)-2-[[*N*-[1-(1*H*-Imidazol-4-yl)-2-propyl]imino](2-hydroxyphenyl)methyl]phenol (9b): method A; crystallized from EtOAc/C_6H_{12}; ^{1}H-NMR (DMSO-d_6) δ 15.77 (br*, 0.64H, NH), 15.65 (br*, 0.36H, NH), 11.75 (br*, 1H, (*E*)-OH), 9.90 (br*, 1H, (*Z*)-OH), 7.49–6.41 (m, 10 H, 8Ph-H, imidazole-2-H, imidazole-5-H), 3.55 (m, 1H, CH), 2.87–2.69 (m, 2H, CH_2), 1.17 (d, 0.64 3H, J = 6.2, CH_3), 1.06 (d, 0.36 3H, J = 6.2, CH_3). Anal. ($C_{19}H_{19}N_3O_2$) C, H, N.

(*R*)-(−)-2-[[*N*-[1-(1*H*-Imidazol-4-yl)-2-propyl]imino]phenylmethyl]resorcinol (9c): method A; crystallized from EtOAc/C_6H_{12}; ^{1}H-NMR (DMSO-d_6) δ 16.13 (s*, 1H, NH), 11.72 (br*, 1H, Ph-2-OH), 9.92 (s*, 1H, Ph-4-OH), 7.48 (m, 4H, Ph-2-H, Ph-4-H, Ph-6-H, imidazole-2-H), 7.23–6.64 (m, 3H, Ph-3, Ph-5-H, imidazole-5-H), 6.33 (d, 1H, J = 8.7, HOPh-3-*H*), 6.17 (s, 1H, HOPh-6-*H*), 6.03 (d, 1H, J = 8.6, HOPh-4-*H*), 3.53 (m, 1H, CH), 2.73 (d, 2H, J = 6, CH_2), 1.15 (d, 3H, J = 6, CH_3). Anal. ($C_{19}H_{19}N_3O_2$) C, H, N.

(*R*)-(−)-2-[[*N*-[1-(1*H*-Imidazol-4-yl)-2-propyl]imino]phenylmethyl]-5-methoxyphenol (9d): method B; crystallized from EtOAc/C_6H_{12}; ^{1}H-NMR (DMSO-d_6) δ 11.73 (br*, 1H, OH), 7.49 (m, 6H, 5Ph-H, imidazole-2-H), 6.63 (s, 1H, imidazole-5-H), 6.41 (d, 1H, J = 8.9, HOPh-3-*H*), 6.33 (s, 1H, HOPh-6-*H*), 6.41 (d, 1H, J = 8.9, HOPh-4-*H*), 3.50 (m, 1H, CH), 2.71 (d, 2H, J = 6.4, CH_2), 2.26 (s, 3H, OCH_3), 1.15 (d, 3H, J = 6.3, CH-C*H*$_3$). Anal. ($C_{20}H_{21}N_3O_2$) C, H, N.

(*R*)-(−)-2-[[*N*-[1-(1*H*-Imidazol-4-yl)-2-propyl]imino]phenylmethyl]-4-methylphenol (9e): method B; crystallized from EtOAc/C_6H_{12}; ^{1}H-NMR (DMSO-d_6) δ 15.32 (s*, 1H, NH), 11.75 (br*, 1H, OH), 7.49 (m, 4H, Ph-2-H, Ph-4-H, Ph-6-H, imidazole-2-H), 7.08 (d, 1H, J = 8.3, HOPh-5-*H*), 6.94 (m, 2H, Ph-3-H, Ph-5-H), 6.79 (d, 1H, J = 8.3, HOPh-6-*H*), 6.61 (s, 1H, imidazole-5-H), 6.34 (s, 1H, HOPh-3-*H*), 3.47 (m, 1H, CH), 2.01 (s, 3H, Ph-CH_3), 2.70 (d, 2H, J = 5.8, CH_2), 1.13 (d, 3H, J = 6.3, CH-C*H*$_3$). Anal. ($C_{20}H_{21}N_3O$) C, H, N.

(*R*)-(−)-4-Fluoro-2-[[*N*-[1-(1*H*-imidazol-4-yl)-2-propyl]imino]phenylmethyl]phenol (9f): method B; crystallized from Et_2O; ^{1}H-NMR (DMSO-d_6) δ 15.32 (s*, 1H, NH), 11.75 (br*, 1H, OH), 7.52 (m, 4H, Ph-2-H, Ph-4-H, Ph-6-H, imidazole-2-H), 7.17 (m, 1H, HOPh-5-*H*), 6.92 (m, 3H, Ph-3-H, Ph-5-H, HOPh-6-*H*), 6.64 (s, 1H, imidazole-5-H), 6.23 (m, 1H, HOPh-3-*H*), 3.53 (m, 1H, CH), 2.72 (d, 2H, J = 5.7, CH_2), 1.15 (d, 3H, J = 6.3, CH_3). Anal. ($C_{19}H_{18}FN_3O$) C, H, N.

(*R*)-(−)-4-Chloro-2-[[*N*-[1-(1*H*-imidazol-4-yl)-2-propyl]imino]phenylmethyl]phenol (9g): method B; crystallized from EtOAc/C_6H_{12}; ^{1}H-NMR (DMSO-d_6) δ 15.81 (s*, 1H, NH), 11.75 (br*, 1H, OH), 7.52 (m, 4H, Ph-2-H, Ph-4-H, Ph-6-H, imidazole-2-H), 7.32 (dd, 1H, ^3J = 8.8, ^4J = 2.7, HOPh-5-*H*), 6.94 (m, 3H, Ph-3-H, Ph-5-H, HOPh-6-*H*), 6.64 (s, 1H, imidazole-5-H), 6.47 (d, 1H, ^4J = 2.7, HOPh-3-*H*), 3.54 (m, 1H, CH), 2.73 (d, 2H, J = 6.3, CH_2), 1.16 (d, 3H, J = 6.4, CH_3). Anal. ($C_{19}H_{18}ClN_3O$) C, H, N.

(*R*)-(−)-4-Bromo-2-[[*N*-[1-(1*H*-imidazol-4-yl)-2-propyl]imino]phenylmethyl]phenol (9h): method B; crystallized from EtOAc/C_6H_{12}; ^{1}H-NMR (DMSO-d_6) δ 15.87 (s*, 1H, NH), 11.80 (br*, 1H, OH), 7.52 (m, 4H, Ph-2-H, Ph-4-H, Ph-6-H, imidazole-2-H), 7.42 (dd, 1H, ^3J = 8.8, ^4J = 2.5, HOPh-5-*H*), 7.01 (m, 2H, Ph-3-H, Ph-5-H), 6.87 (d, 1H, ^3J = 8.8, HOPh-6-*H*), 6.65 (s, 1H, imidazole-5-H), 6.60 (d, 1H, ^4J = 2.5, HOPh-

3-*H*), 3.54 (m, 1H, CH), 2.73 (d, 2H, J = 6.3, CH_2), 1.16 (d, 3H, J = 6.3, CH_3). Anal. ($C_{19}H_{18}BrN_3O$) C, H, N.

(*R*)-(−)-4-Chloro-2-[[*N*-[1-(1*H*-imidazol-4-yl)-2-propyl]-imino]phenylmethyl]-5-methylphenol (9i): method A; crystallized from EtOAc/C_6H_{12}; ^{1}H-NMR (DMSO-d_6) δ 15.68 (s*, 1H, NH), 11.75 (br*, 1H, OH), 7.50 (m, 4H, Ph-2-H, Ph-4-H, Ph-6-H, imidazole-2-H), 6.98 (br, 2H, Ph-3-H), 6.91 (s, 1H, HOPh-6-*H*), 6.62 (s, 1H, imidazole-5-H), 6.44 (s, 1H, HOPh-3-*H*), 3.50 (m, 1H, CH), 2.71 (d, 2H, J = 6.4, CH_2), 2.26 (s, 3H, Ph-CH_3), 1.15 (d, 3H, J = 6.3, CH-CH_3). Anal. ($C_{20}H_{20}ClN_3O$·0.5H_2O) C, H, N.

(*R*)-(−)-6-Chloro-4-fluoro-2-[[*N*-[1-(1*H*-imidazol-4-yl)-2-propyl]imino]phenylmethyl]phenol (9k): method B; crystallized from EtOAc/C_6H_{12}; ^{1}H-NMR (DMSO-d_6) δ 16.87 (s*, 1H, NH), 11.80 (br*, 1H, OH), 7.53 (m, 5H, Ph-2-H, Ph-4-H, Ph-6-H, HOPh-5-*H*, imidazole-2-H), 7.06 (m, 2H, Ph-3-H, Ph-5-H), 6.69 (s, 1H, imidazole-5-H), 6.21 (dd, 1H, $^3J_{H,F}$ = 9.6, $^4J_{H,H}$ = 3.1, HOPh-3-*H*), 3.61 (m, 1H, CH), 2.77 (d, 2H, J = 7.3, CH_2), 1.21 (d, 3H, J = 6.3, CH_3). Anal. ($C_{19}H_{17}ClFN_3O$) C, H, N.

(*R*)-(−)-2-[[*N*-[1-(1*H*-Imidazol-4-yl)-2-propyl]imino](4-fluorophenyl)methyl]phenol (9l): method B; crystallized from EtOAc/C_6H_{12}; ^{1}H-NMR (DMSO-d_6) δ 15.49 (s*, 1H, NH), 7.54 (s, 1H, imidazole-2-H), 7.30 (m, 3H, FPh-2-H, FPh-6-H, HOPh-5-*H*), 6.95 (m, 3H, FPh-3-H, FPh-5-H, HOPh-6-*H*), 6.61 (m, 3H, HOPh-3-*H*, HOPh-4-*H*, imidazole-5-H), 3.50 (m, 1H, CH), 2.72 (d, 2H, J = 6.3, CH_2), 1.16 (d, 3H, J = 6.2, CH_3). Anal. ($C_{19}H_{18}FN_3O$) C, H, N.

(*R*)-(−)-2-[[*N*-[1-(1*H*-Imidazol-4-yl)-2-propyl]imino](4-chlorophenyl)methyl]phenol (9m): method B; crystallized from Et_2O; ^{1}H-NMR (DMSO-d_6) δ 15.51 (s*, 0.6H, NH), 15,24 (s*, 0.4H, NH), 11.73 (br*, 1H, OH), 7.55 (d, 2H, ^3J = 8.4, ClPh-2-H, ClPh-6-H), 7.49 (s, 1H, imidazole-2-H), 7.28−6.48 (m, 7H, ClPh-3-H, ClPh-5-H, 4HOPh-*H*, imidazole-5-H), 3.52 (m, 1H, CH), 2.75 (d, 0.4 2H, J = 6.2, CH_2), 2.69 (d, 0.6 2H, J = 6.2, CH_2), 1.18 (d, 0.4 3H, J = 6.2, CH_3), 1.14 (d, 0.6 3H, J = 6.2, CH_3). Anal. ($C_{19}H_{18}ClN_3O$) C, H, N.

(*R*)-(−)-4-Fluoro-2-[[*N*-[1-(1*H*-imidazol-4-yl)-2-propyl]-imino](4-fluorophenyl)methyl]phenol (9n): method B; crystallized from EtOAc/C_6H_{12}; ^{1}H-NMR (DMSO-d_6) δ 15.22 (s*, 1H, NH), 7.51 (s, 1H, imidazole-2-H), 7.35 (m, 2H, FPh-2-H, FPh-6-H), 7.18 (m, 1H, HOPh-5-*H*), 7.05 (m, 2H, FPh-3-H, FPh-5-H), 6.92 (dd, 1H, $^3J_{H,H}$ = 9, $^4J_{H,F}$ = 4.8, HOPh-6-*H*), 6.65 (s, imidazole-5-H), 6.25 (dd, 1H, $^3J_{H,F}$ = 9.8, $^4J_{H,H}$ = 2.8, HOPh-3-*H*), 3.52 (m, 1H, CH), 2.72 (d, 2H, J = 6.2, CH_2), 1.16 (d, 3H, J = 6.2, CH_3). Anal. ($C_{19}H_{17}F_2N_3O$) C, H, N.

(*R*)-(−)-4-Chloro-2-[[*N*-[1-(1*H*-imidazol-4-yl)-2-propyl]-imino](4-fluorophenyl)methyl]phenol (9o): method B; crystallized from EtOAc/C_6H_{12}; ^{1}H-NMR (DMSO-d_6) δ 15.12 (s*, 1H, NH), 11.75 (br*, 1H, OH), 7.50 (s, 1H, imidazole-2-H), 7.35 (m, 3H, FPh-2-H, FPh-6-H, HOPh-5-*H*), 6.95 (m, 3H, FPh-3-H, FPh-5-H, HOPh-6-*H*), 6.65 (s, 1H, imidazole-5-H), 6.49 (d, 1H, ^4J = 2.7, HOPh-3-*H*), 3.52 (m, 1H, CH), 2.73 (d, 2H, J = 6.4, CH_2), 1.17 (d, 3H, J = 6.3, CH_3). Anal. ($C_{19}H_{17}ClFN_3O$) C, H, N.

(*R*)-(−)-4-Fluoro-2-[[*N*-[1-(1*H*-imidazol-4-yl)-2-propyl]-imino](4-chlorophenyl)methyl]phenol (9p): method B; crystallized from EtOAc/C_6H_{12}; ^{1}H-NMR (DMSO-d_6) δ 15.12 (s*, 1H, NH), 11.73 (br*, 1H, OH), 7.57 (d, 2H, ^3J = 8.7, ClPh-2-H, ClPh-6-H), 7.50 (s, 1H, imidazole-2-H), 7.22 (m, 1H, HOPh-5-*H*), 6.93 (m, 3H, ClPh-3-H, ClPh-5-H, HOPh-6-*H*), 6.64 (s, imidazole-5-H), 6.25 (dd, 1H, $^3J_{H,F}$ = 9.8, $^4J_{H,H}$ = 3, HOPh-3-*H*), 3.50 (m, 1H, CH), 2.72 (d, 2H, J = 6.3, 2H, CH_2), 1.18 (d, 3H, J = 6.2, CH_3). Anal. ($C_{19}H_{17}ClFN_3O$) C, H, N.

(*R*)-(−)-4-Chloro-2-[[*N*-[1-(1*H*-Imidazol-4-yl)-2-propyl]-imino](4-chlorophenyl)methyl]phenol (9q): method B; crystallized from EtOAc/C_6H_{12}; ^{1}H-NMR (DMSO-d_6) δ 15.62 (s*, 1H, NH), 11.76 (br*, 1H, OH), 7.59 (d, 2H, ^3J = 8.7, ClPh-2-H, ClPh-6-H), 7.50 (s, 1H, imidazole-2-H), 7.34 (dd, 1H, ^3J = 8.8, ^4J = 2.6, HOPh-5-*H*), 6.95 (m, 3H, ClPh-3-H, ClPh-5-H, HOPh-6-*H*), 6.65 (s, 1H, imidazole-5-H), 6.49 (d, 1H, ^4J = 2.6, HOPh-3-*H*), 3.50 (m, 1H, CH), 2.73 (d, 2H, J = 5.3, CH_2), 1.17 (d, 3H, J = 6.3, CH_3). Anal. ($C_{19}H_{17}Cl_2N_3O$) C, H, N.

(*R*)-(−)-4-Fluoro-2-[[*N*-[1-(1*H*-Imidazol-4-yl)-2-propyl]-imino](1-naphthyl)methyl]phenol (9r): method B; refluxed for 240 h; crystallized from EtOAc/light petroleum; ^{1}H-NMR (DMSO-d_6) δ 15.31 (s*, 0.6H, NH), 15.29 (s*, 0.4H, NH), 8.12−6.62 (m, 9H, aryl-H), 6.00 (m, 1H, aryl-H), 3.36 (m, 1H, CH), 2.72 (m, 2H, CH_2), 1.17 (d, 0.5 3H, J = 6.3, CH_3), 1.07 (d, 0.5 3H, J = 6.2, CH_3).[51] Anal. ($C_{23}H_{20}FN_3O$·0.25H_2O) C, H, N.

6-(*R*)-(−)-6-Methyl-4-phenyl-4,5,6,7-tetrahydro-1*H*-imidazo[4,5-*c*]pyridine (11a). 1 and benzaldehyde yielded **11a** according to method A described for the azomethines. The white solid obtained was recrystallized from MeOH/Et_2O: ^{1}H-NMR (DMSO-d_6) δ 11.74 (s*, 0.5H, NH), 11.40 (s*, 0.5H, NH), 7.26 (m, 6H, 5Ph-H, imidazole-2-H), 4.94 (s, 0.5H, Ph-C*H*), 4.85 (s, 0.5H, Ph-C*H*), 3.36 (br, 1H, C*H*-CH_3), 2.51−2.33 (m, 2H, CH_2), 1.17 (d, 3H, J = 5.6, CH_3). Anal. ($C_{13}H_{15}N_3$·0.5H_2O) C, H, N.

6-(*R*)-(+)-4-(2-Hydroxyphenyl)-6-methyl-4,5,6,7-tetrahydro-1*H*-imidazo[4,5-*c*]pyridine (11b). 1 and salicylaldehyde yielded **11b** according to method A described for the azomethines. The white solid obtained was recrystallized from EtOH/Et_2O: ^{1}H-NMR (DMSO-d_6) δ 11.79 (br*, 1H, NH), 7.34 (s, 1H, imidazole-2-H), 7.22 (d, 1H, J = 7, Ph-6-H), 7.08 (m, 1H, Ph-4-H), 6.76 (m, 1H, Ph-5-H), 6.62 (d, 1H, J = 7, Ph-3-H), 5.07 (s, 1H, Ph-C*H*), 3.04 (m, 1H, C*H*-CH_3), 2.55 (m, 1H, C*H*-H′), 2.36 (m, 1H, CH-*H*′), 1.24 (d, 3H, J = 6.2, CH_3). Anal. ($C_{13}H_{15}N_3O$) C, H, N.

6-(*R*)-(+)-4-(2-Hydroxyphenyl)-6,4-dimethyl-4,5,6,7-tetrahydro-1*H*-imidazo[4,5-*c*]pyridine (11c). 1 and 2-hydroxyacetophenone yielded **11c** according to method A described for the azomethines. The white solid obtained was recrystallized from EtOH/Et_2O: ^{1}H-NMR (DMSO-d_6) δ 13.58 (br*, 1H, NH), 11.68 (br*, 1H, OH), 7.43 (d, 1H, J = 7.6, Ph-6-H), 7.33 (s, 1H, imidazole-2-H), 7.02 (m, 1H, Ph-4-H), 6.71 (m, 1H, Ph-5-H), 6.50 (d, 1H, J = 7.8, Ph-3-H), 3.34 (m, 1H, CH), 2.63−2.36 (m, 2H, CH_2), 1.71 (m, 3H, C-CH_3), 1.20 (d, 3H, J = 6.0, CH-CH_3). Anal. ($C_{14}H_{17}N_3O$·H_2O) C, H, N.

Single Crystal X-ray Analyses of 9a,p. The X-ray analyses were executed in the same way for **9a**,**p**. Precise lattice parameters and three-dimensional intensity data were measured on a Stoe diffractometer using Ni-filtered Cu Kα radiation (λ = 1.5418 Å). The intensity data sets were corrected for Lorentz and polarization effects but not for absorption. Phase determination was made with direct methods (program SHELXS86);[47] refinement was done with the corresponding least-squares programs of the XTAL program system (version 3.2, 1992).[48] All hydrogen atoms were located from difference syntheses. A $1/\sigma^2(F_o)$ weighting scheme was used; $\sigma(F_o)$ was from counting statistics. No significant peaks or holes were seen in final difference Fourier maps.

Crystal Data of 9a. Crystals of **9a**, molecular formula $C_{19}H_{19}N_3O$ (M_r = 305.4), were grown from EtOAc/light petroleum (bp 50−70 °C): space group, orthorhombic $P2_12_12_1$; unit cell, a = 17.475(5) Å, b = 9.787(2) Å, c = 9.630(2) Å, V = 1647.0(7) Å^3, Z = 4, ϱ_x = 1.232 g cm^{-3}, μ(Cu Kα) = 6.28 cm^{-1}. A single crystal with dimensions 0.46 × 0.40 × 0.40 mm^3 was used to collect the intensity data of 1573 independent reflections ($\theta \leq 64°$; h, k, l all ≥ 0) by using the $\omega-2\theta$ scan technique. An intensity variation of less than 2.5%, monitored via three check reflections, was considered insignificant. A total of 290 reflections with $F_o \leq \sigma(F_o)$ were coded unobserved. After convergence, R values of R = 4.1% and R_w = 2.8% were obtained.

Crystal Data of 9p. Crystals of **9p**, molecular formula $C_{19}H_{17}ClFN_3O$ (M_r = 357.8), were grown from EtOAc/light petroleum (bp 50−70 °C): space group, orthorhombic $P2_12_12_1$; unit cell, a = 20.403(3) Å, b = 9.517(2) Å, c = 9.247(2) Å, V = 1795.5(6) Å^3, Z = 4, ϱ_x = 1.321 g cm^{-3}, μ(Cu Kα) = 20.75 cm^{-1}. A single crystal with dimensions 0.63 × 0.45 × 0.45 mm^3 was used to collect the intensity data of 1720 independent reflections ($\theta \leq 64°$; h, k, l all ≥ 0) by using the $\omega-2\theta$ scan technique. An intensity variation of less than 6%, monitored via three check reflections, was considered insignificant. A total of 58 reflections with $F_o \leq 2\sigma(F_o)$ were coded unobserved. After convergence, R values of R = 3.1% and R_w = 3.4% were obtained.

Pharmacology. Materials and Methods. Determination of Prodrug Hydrolysis Rates *in Vitro*. A 10 mM prodrug solution prepared extemporaneously in DMSO was diluted to a final concentration of 4 μM in 0.4 N $HClO_4$ or in 0.05 M K_2HPO_4/KH_2PO_4 buffer, pH 7.4, and incubated at room

temperature. At various time intervals, an aliquot was taken, diluted, and brought up to a final concentration of 0.4 N $HClO_4$. Immediately after the incubation, 1 was measured by a sensitive and specific RIA developed according to a principle already described.[49] Briefly, perchloric samples or standards were derivatized with *p*-benzoquinone during a 30 min incubation at room temperature. The derivatized samples were then incubated with an antiserum raised in rabbits for 1 h at 37 °C and left at 4 °C overnight after transfer in swine anti-rabbit IgG-coated 96-well plates and addition of an [^{125}I]iodinated tracer. The radioactivity bound to the wells was then counted in a γ-spectrometer with an efficiency of 82%. The hydrolysis rate of the prodrug was calculated as the percent ratio of the level of 1 measured in the sample and that corresponding to a complete hydrolysis of the prodrug.

Determination of 1 and Prodrug Levels in Plasma and Cerebral Cortex of Mice Treated with the Various Prodrugs. Male Swiss mice (20–25 g; Iffa-Credo, France) that were given food and water *ad libitum* received an oral dose of 24 μmol/kg prodrug in 1% methyl cellulose and were sacrificed by decapitation 0.5, 1, 3, or 6 h later. Controls received the vehicle only. For determination of 1 and prodrug levels in plasma and cerebral cortex, blood was collected after decapitation and centrifuged (15000*g* for 1 min), and the cerebral cortex was dissected out rapidly and homogenized in 10 vol (w/v) of ice-cold 0.4 N $HClO_4$. Plasma and cerebral extracts were then centrifuged, and the clear supernatant was used for the RIA immediately or stored at −20 °C. Before use one aliquot of the $HClO_4$ extract was heated at 95 °C for 30 min to allow the total *in vitro* hydrolysis of the prodrug. Another one was used without heating. Compound 1 was derivatized and radioimmunoassayed in the nonheated and heated extracts. The prodrug level was calculated as the difference between these two determinations. The plasma from nontreated mice was also assayed in order to estimate the interference of plasma in the RIA for 1. The determinations of 1 for treated mice were then corrected accordingly.

Acknowledgment. We greatly acknowledge the gift of (*R*)-α-methylhistamine kindly provided by Dr. J.-M. Lecomte (Bioprojet, Paris, France). This work was supported by the Biomedical Health and Research Programme BIOMED I of the European Community (EEC BMHT1 CT92-1087) and by the Verband der Chemischen Industrie, Fonds der Chemie (Frankfurt/Main, Germany).

Supporting Information Available: X-ray data including atomic coordinates, distances and angles, and hydrogen bond distances (12 pages); tables of observed and calculated structure factors (4 pages). Ordering information is given on any current masthead page.

References

(1) Arrang, J.-M.; Garbarg, M.; Schwartz, J.-C. Auto-Inhibition of Brain Histamine Release Mediated by a Novel Class (H3) of Histamine Receptor. *Nature (London)* **1983**, *302*, 832–837.
(2) Arrang, J.-M.; Garbarg, M.; Lancelot, J.-C.; Lecomte, J.-M.; Pollard, H.; Robba, M.; Schunack, W.; Schwartz, J.-C. Highly Potent and Selective Ligands for Histamine H_3-Receptors. *Nature (London)* **1987**, *327*, 117–123.
(3) Lipp, R.; Stark, H.; Schunack, W. Pharmacochemistry of H_3-Receptors. In *The Histamine Receptor, Receptor Biochemistry and Methodology*; Schwartz, J.-C., Haas, H. L., Eds.; Wiley-Liss, Inc.: New York, 1992; pp 57–72.
(4) Arrang, J.-M.; Garbarg, M.; Schwartz, J.-C. Autoregulation of Histamine Release in Brain by Presynaptic H_3-Receptors. *Neuroscience* **1985**, *15*, 553–562.
(5) Arrang, J.-M.; Garbarg, M.; Schwartz, J.-C. Autoinhibition of Histamine Synthesis Mediated by Presynaptic H_3-Receptors. *Neuroscience* **1987**, *23*, 149–157.
(6) Fink, K.; Schlicker, E.; Göthert, M. Modulation of N-Methyl-D-Aspartate (NMDA)-stimulated Noradrenaline Release in Rat Brain Cortex by Presynaptic α_2-Adrenoceptors and Histamine H_3-Receptors. *Adv. Biosci.* **1991**, *82*, 125–126.
(7) Clapham, J.; Kilpatrick, G. J. Histamine H_3 Receptors Modulate the Release of [^{3}H]-Acetylcholine from Slices of Rat Entorhinal Cortex: Evidence for the Possible Existence of H_3 Receptor Subtypes. *Br. J. Pharmacol.* **1992**, *107*, 919–923.
(8) Schlicker, E.; Fink, K.; Detzner, M.; Göthert, M. Histamine Inhibits Dopamine Release in the Mouse Striatum via Presynaptic H_3 Receptors. *J. Neural Transm., Gen. Sect.* **1993**, *93*, 1–10.
(9) Schlicker, E.; Betz, R.; Göthert, M. Histamine H_3 Receptor Mediated Inhibition of Serotonin Release in the Rat Brain Cortex. *Naunyn-Schmiedeberg's Arch. Pharmacol.* **1988**, *337*, 588–590.
(10) Burgaud, J. L.; Oudart, N. Effect of an Histaminergic H_3 Agonist on the Non-adrenergic Non-cholinergic Contraction in the Guinea-pig Perfused Bronchioles. *J. Pharm. Pharmacol.* **1993**, *45*, 955–958.
(11) Devillier, P.; Arrang, J.-M.; Garbarg, M.; Pollard, H.; Schwartz, J.-C. The Third Histamine Receptor: Pharmacology and Therapeutic Perspectives. *Médecine/Sciences* **1989**, *5*, 408–414.
(12) Pollard, H.; Moreau, J.; Arrang, J.-M.; Schwartz, J.-C. A Detailed Auto-radiographic Mapping of H_3 Receptors in Rat Brain Areas. *Neuroscience* **1993**, *52*, 169–189.
(13) Ligneau, X.; Garbarg, M.; Vizuette, M. L.; Diaz, J.; Purand, K.; Stark, H.; Schunack, W.; Schwartz, J.-C. [^{125}I]Iodoproxyfan, a New Antagonist to Label and Visualize Cerebral H_3 Receptors. *J. Pharmacol. Exp. Ther.* **1994**, *271*, 452–459.
(14) Arrang, J.-M.; Devaux, B.; Chodkiewicz, J.-P.; Schwartz, J.-C. H_3 Receptors Control Histamine Release in Human Brain. *J. Neurochem.* **1988**, *51*, 105–108.
(15) Gerhard, G.; Schunack, W. Structure-Activity Relationships of Histamine Analogues. XX. Absolute Configuration and Histamine-like Activity of Enantiomeric α-Methylhistamines. *Arch. Pharm. (Weinheim)* **1980**, *313*, 709–714.
(16) Rouleau, A. *et al.* Unpublished results.
(17) Lin, J. S.; Sakai, K.; Vanni-Mercier, G.; Arrang, J.-M.; Garbarg, M.; Schwartz, J.-C.; Jouvet, M. Involvement of Histaminergic Neurons in Arousal Mechanisms Demonstrated with H_3-Receptor Ligands in the Cat. *Brain Res.* **1990**, *523*, 325–330.
(18) Ichinose, M.; Beloisi, M. G.; Barnes, P. J. Histamine H_3-Receptors Inhibit Neurogenic Microvascular Leakage in Airways. *J. Appl. Physiol.* **1990**, *68*, 21–25.
(19) Barnes, P. J. Histamine Receptors in the Respiratory Tract. In *The Histamine Receptor, Receptor Biochemistry and Methodology*; Schwartz, J.-C., Haas, H. L., Eds.; Wiley-Liss, Inc.: New York, 1992; pp 253–270.
(20) Yamazaki, S.; Sakurai, E.; Hikichi, N.; Sakai, N.; Maeyama, K.; Watanabe, T. The Disposition of (*R*)-α-Methylhistamine, a Histamine H_3-Receptor Agonist, in Rats. *J. Pharm. Pharmacol.* **1994**, *46*, 371–374.
(21) Schayer, R. W.; Reilly, M. A. In Vivo Formation and Catabolism of ^{14}C-Histamine in Mouse Brain. *J. Neurochem.* **1970**, *17*, 1649–1655.
(22) Schwartz, J.-C.; Pollard, H.; Bischoff, S.; Rehault, M. C.; Verdiere, M. Catabolism of ^{3}H-Histamine in the Rat Brain after Intracisternal Administration. *Eur. J. Pharmacol.* **1971**, *16*, 326–335.
(23) Cooper, D. G.; Young, R. C.; Durant, G. J.; Ganellin, C. R. Histamine Receptors. In *Comprehensive Medicinal Chemistry: the Rational Design, Mechanistic Study & Therapeutic Application of Chemical Compounds*; Hansch, C., Ed.; Pergamon Press: Oxford, U.K., 1990; pp 323–421.
(24) Hough, L. B.; Khandelwal, J. K.; Mittag, T. W. Alpha-Methylhistamine Methylation by Histamine Methyltransferase. *Agents Actions* **1981**, *11*, 425–428.
(25) Garbarg, M.; Arrang, J.-M.; Schunack, W.; Lipp, R.; Stark, H.; Lecomte, J.-M.; Schwartz, J.-C. PCT Int. Appl. WO 91/17 146, November 11, 1991.
(26) Kaplan, J.-P.; Raizon, B. M.; Desarmien, M.; Feltz, P.; Headly, P. M.; Worms, P.; Lloyd, K. G.; Bartholini, G. New Anticonvulsants: Schiff Bases of γ-Aminobutyric Acid and γ-Aminobutyramide. *J. Med. Chem.* **1980**, *23*, 702–704.
(27) Bergmann, K. J. Progabide: a New GABA-Mimetic Agent in Clinical Use. *Clin. Neuropharmacol.* **1985**, *8*, 13–26.
(28) Raizon, B.; Rossey, G.; Wick, A. Diphenylazomethines. Eur. Pat. Appl. EP 193,450, September 3, 1986; *Chem. Abstr.* **1986**, *105*, P226012d.
(29) Jílek, J.; Pomykácek, J.; Frycová, H.; Polívka, Z. Synthesis of Analogues of Progabide and Fengabine. *Cesk. Farm.* **1990**, *39*, 249–253.
(30) Green, T. W.; Wuts, P. G. M. *Protective Groups in Organic Chemistry*, 2nd ed.; John Wiley & Sons, Inc.: New York, 1991; pp 368–371.
(31) Fries, K.; Finck, G. About Homologues of Cumaranon and Their Derivatives. *Ber. Dtsch. Chem. Ges.* **1908**, *41*, 4271.
(32) Gerecs, A. The Fries Reaction. In *Friedel-Crafts and Related Reactions*; Olah, G. A., Ed.; Interscience Publishers: New York, 1964; Vol. III, pp 499–533.
(33) Einhorn, A.; Hollandt, F. About Acylation of Alcohols and Phenols in Pyridine Solution. *Ann. Chem.* **1898**, *301*, 95–101.
(34) Suter, C. M.; Lawson, E. J.; Smith, P. G. The Synthesis and Germicidal Properties of Some Alkylfluorophenols. *J. Am. Chem. Soc.* **1939**, *61*, 161–165.

(35) Nunn, L. G.; Henze, H. R. Certain 1-Naphthyl Ketones. *J. Org. Chem.* **1947**, *12*, 540–542.
(36) McOmie, J. F. W.; Watts, M. L.; West, D. E. Demethylation of Aryl Methyl Ethers by Boron Tribromide. *Tetrahedron* **1968**, *24*, 2289–2292.
(37) Whaley, W. M.; Govindachari, T. R. The Pictet-Spengler Synthesis of Tetrahydroisoquinolines and Related Compounds. In *Organic Reactions*; Adams, R., Ed.; John Wiley and Sons, Inc.: New York, 1951; Vol. VI, pp 151–190.
(38) Heyl, D.; Luz, E.; Harris, S. A.; Folkers, K. Chemistry of Vitamin B_6. VII. Pyridoxylidene- and Pyridoxylamines. *J. Am. Chem. Soc.* **1948**, *70*, 3669–3671.
(39) Stocker, F. B.; Fordice, M. W.; Larson, J. K.; Thorstenson, J. H. Some 4-Aryl-4,5,6,7-tetrahydroimidazo[4,5-c]pyridines Derived from Histamine. *J. Org. Chem.* **1966**, *31*, 2380–2383.
(40) Emmett, J. C.; Durant, G. J.; Ganellin, C. R.; Roe, A. M.; Turner, J. T. Potential Histamine H_2-Receptor Antagonists. 4. Benzylhistamines. *J. Med. Chem.* **1982**, *25*, 1168–1174.
(41) Keller, E. *SCHAKAL86, Program for the Graphic Representation of Molecular and Crystallographic Models*; University of Freiburg: Germany, 1986.
(42) Lipp, R.; Arrang, J.-M.; Garbarg, M.; Luger, P.; Schwartz, J.-C.; Schunack, W. Synthesis, Absolute Configuration, Stereoselectivity, and Receptor Selectivity of (αR,βS)-α,β-Dimethylhistamine, a Novel Highly Potent Histamine H_3 Receptor Agonist. *J. Med. Chem.* **1992**, *35*, 4434–4441.
(43) Bonnet, J. J.; Ibers, J. A. The Structure of Histamine. *J. Am. Chem. Soc.* **1973**, *95*, 4829–4833.
(44) Garbarg, M.; Arrang, J.-M.; Rouleau, A.; Ligneau, X.; Dam Trung Tuong, M.; Schwartz, J.-C.; Ganellin, C. R. S-[2-(4-Imidazolyl) ethyl]isothiourea, a Highly Specific and Potent Histamine H_3 Receptor Agonist. *J. Pharmacol. Exp. Ther.* **1992**, *263*, 304–310.
(45) Lipp, R.; Stark, H.; Arrang, J.-M.; Garbarg, M.; Schwartz, J.-C.; Schunack, W. Synthesis and Histamine H_3-Receptor Agonist Activity of Mono- and Dialkyl Substituted Histamine Derivatives. *Eur. J. Med. Chem.* **1995**, *30*, 219–225.
(46) Stark, H.; Arrang, J.-M.; Garbarg, M.; Rouleau, A.; Lecomte, J.-M.; Lipp, R.; Schwartz, J.-C.; Schunack, W. Prodrugs of Histamine H_3-Agonists for Improved Drug Penetration through Blood-Brain Barrier. Presented at the XIIth International Symposium on Medicinal Chemistry, Basel, Switzerland, September 13–17, 1992.
(47) Sheldrick, G. M. In *Crystallographic Computing 3*; Sheldrick, G. M., Krüger, C., Goddard, R., Eds.; Oxford University Press: Oxford, U.K., 1985; pp 175–198.
(48) Stewart, J. M., Flack, H. D., Hall, S. R., Eds. *XTAL Program System 3.2, User's Manual*; University of Western Australia, Geneva, and Maryland, 1992.
(49) Garbarg, M.; Pollard, H.; Trung Tuong, M. D.; Schwartz, J.-C.; Gros, C. Sensitive Radioimmunoassays for Histamine and Tele-Methylhistamine in the Brain. *J. Neurochem.* **1989**, *53*, 1724–1730.
(50) Black, J. W.; Ganellin, C. R. Naming Substituted Histamines. *Experientia* **1974**, *30*, 111–113.
(51) The existence of two atropisomers of **9r** is suggested as the voluminous naphthyl ring should not be able to rotate freely around the N=C–naphthyl σ bond. In addition to ^{1}H-NMR analysis, we have investigated this compound by ^{13}C-NMR and X-ray crystallography, but unfortunately this suggestion could not have been finally confirmed yet. Investigations on this problem are still in progress.

JM950301X